

A flavour-independent Higgs boson search in e^+e^- collisions at \sqrt{s} up to 209 GeV

The ALEPH Collaboration*)

Abstract

A search for the Higgsstrahlung process $e^+e^- \rightarrow HZ$ is carried out, covering decays of the Higgs boson into any quark pair, a gluon pair or a tau pair. The analysis is based on the 630 pb^{-1} of data collected by the ALEPH detector at LEP at centre-of-mass energies from 189 to 209 GeV. A 95% C.L. lower mass limit of $109.1 \text{ GeV}/c^2$ is obtained for a Higgs boson cross section equal to that expected from the Standard Model if the Higgs boson decays exclusively into hadrons and/or taus, irrespective of the relative branching fractions.

Submitted to Physics Letters B

*) See next pages for the list of authors

The ALEPH Collaboration

A. Heister, S. Schael

Physikalisches Institut des RWTH-Aachen, D-52056 Aachen, Germany

R. Barate, R. Brunelière, I. De Bonis, D. Decamp, C. Goy, S. Jezequel, J.-P. Lees, F. Martin, E. Merle, M.-N. Minard, B. Pietrzyk, B. Trocmé

Laboratoire de Physique des Particules (LAPP), IN²P³-CNRS, F-74019 Annecy-le-Vieux Cedex, France

G. Boix,²⁵ S. Bravo, M.P. Casado, M. Chmeissani, J.M. Crespo, E. Fernandez, M. Fernandez-Bosman, Ll. Garrido,¹⁵ E. Graugés, J. Lopez, M. Martinez, G. Merino, R. Miquel,⁴ Ll.M. Mir,⁴ A. Pacheco, D. Paneque, H. Ruiz

Institut de Física d'Altes Energies, Universitat Autònoma de Barcelona, E-08193 Bellaterra (Barcelona), Spain⁷

A. Colaleo, D. Creanza, N. De Filippis, M. de Palma, G. Iaselli, G. Maggi, M. Maggi, S. Nuzzo, A. Ranieri, G. Raso,²⁴ F. Ruggieri, G. Selvaggi, L. Silvestris, P. Tempesta, A. Tricomi,³ G. Zito

Dipartimento di Fisica, INFN Sezione di Bari, I-70126 Bari, Italy

X. Huang, J. Lin, Q. Ouyang, T. Wang, Y. Xie, R. Xu, S. Xue, J. Zhang, L. Zhang, W. Zhao

Institute of High Energy Physics, Academia Sinica, Beijing, The People's Republic of China⁸

D. Abbaneo, P. Azzurri, T. Barklow,³⁰ O. Buchmüller,³⁰ M. Cattaneo, F. Cerutti, B. Clerbaux,³⁴ H. Drevermann, R.W. Forty, M. Frank, F. Gianotti, T.C. Greening,²⁶ J.B. Hansen, J. Harvey, D.E. Hutchcroft, P. Janot, B. Jost, M. Kado,² P. Mato, A. Moutoussi, F. Ranjard, L. Rolandi, D. Schlatter, G. Sguazzoni, W. Tejessy, F. Teubert, A. Valassi, I. Videau, J.J. Ward

European Laboratory for Particle Physics (CERN), CH-1211 Geneva 23, Switzerland

F. Badaud, S. Dessagne, A. Falvard,²⁰ D. Fayolle, P. Gay, J. Jousset, B. Michel, S. Monteil, D. Pallin, J.M. Pascolo, P. Perret

Laboratoire de Physique Corpusculaire, Université Blaise Pascal, IN²P³-CNRS, Clermont-Ferrand, F-63177 Aubière, France

J.D. Hansen, J.R. Hansen, P.H. Hansen, B.S. Nilsson

Niels Bohr Institute, 2100 Copenhagen, DK-Denmark⁹

A. Kyriakis, C. Markou, E. Simopoulou, A. Vayaki, K. Zachariadou

Nuclear Research Center Demokritos (NRCD), GR-15310 Attiki, Greece

A. Blondel,¹² J.-C. Brient, F. Machefert, A. Rougé, M. Swynghedauw, R. Tanaka
H. Videau

Laboratoire de Physique Nucléaire et des Hautes Energies, Ecole Polytechnique, IN²P³-CNRS, F-91128 Palaiseau Cedex, France

V. Ciulli, E. Focardi, G. Parrini

Dipartimento di Fisica, Università di Firenze, INFN Sezione di Firenze, I-50125 Firenze, Italy

A. Antonelli, M. Antonelli, G. Bencivenni, F. Bossi, G. Capon, V. Chiarella, P. Laurelli, G. Mannocchi,⁵ G.P. Murtas, L. Passalacqua

Laboratori Nazionali dell'INFN (LNF-INFN), I-00044 Frascati, Italy

J. Kennedy, J.G. Lynch, P. Negus, V. O'Shea, A.S. Thompson

Department of Physics and Astronomy, University of Glasgow, Glasgow G12 8QQ, United Kingdom¹⁰

S. Wasserbaech

Department of Physics, Haverford College, Haverford, PA 19041-1392, U.S.A.

R. Cavanaugh,³³ S. Dhamotharan,²¹ C. Geweniger, P. Hanke, V. Hepp, E.E. Kluge, G. Leibenguth, A. Putzer, H. Stenzel, K. Tittel, M. Wunsch¹⁹

Kirchhoff-Institut für Physik, Universität Heidelberg, D-69120 Heidelberg, Germany¹⁶

R. Beuselinck, W. Cameron, G. Davies, P.J. Dornan, M. Girone,¹ R.D. Hill, N. Marinelli, J. Nowell, S.A. Rutherford, J.K. Sedgbeer, J.C. Thompson,¹⁴ R. White

Department of Physics, Imperial College, London SW7 2BZ, United Kingdom¹⁰

V.M. Ghete, P. Girtler, E. Kneringer, D. Kuhn, G. Rudolph

Institut für Experimentalphysik, Universität Innsbruck, A-6020 Innsbruck, Austria¹⁸

E. Bouhova-Thacker, C.K. Bowdery, D.P. Clarke, G. Ellis, A.J. Finch, F. Foster, G. Hughes, R.W.L. Jones, M.R. Pearson, N.A. Robertson, M. Smizanska

Department of Physics, University of Lancaster, Lancaster LA1 4YB, United Kingdom¹⁰

O. van der Aa, C. Delaere, V. Lemaitre

Institut de Physique Nucléaire, Département de Physique, Université Catholique de Louvain, 1348 Louvain-la-Neuve, Belgium

U. Blumenschein, F. Hölldorfer, K. Jakobs, F. Kayser, K. Kleinknecht, A.-S. Müller, G. Quast,⁶ B. Renk, H.-G. Sander, S. Schmeling, H. Wachsmuth, C. Zeitnitz, T. Ziegler

Institut für Physik, Universität Mainz, D-55099 Mainz, Germany¹⁶

A. Bonissent, P. Coyle, C. Curtil, A. Ealet, D. Fouchez, P. Payre, A. Tilquin

Centre de Physique des Particules de Marseille, Univ Méditerranée, IN²P³-CNRS, F-13288 Marseille, France

F. Ragusa

Dipartimento di Fisica, Università di Milano e INFN Sezione di Milano, I-20133 Milano, Italy.

A. David, H. Dietl, G. Ganis,²⁷ K. Hüttmann, G. Lütjens, W. Männer, H.-G. Moser, R. Settles, G. Wolf

Max-Planck-Institut für Physik, Werner-Heisenberg-Institut, D-80805 München, Germany¹⁶

J. Boucrot, O. Callot, M. Davier, L. Duflot, J.-F. Grivaz, Ph. Heusse, A. Jacholkowska,³² C. Loomis, L. Serin, J.-J. Veillet, J.-B. de Vivie de Régie,²⁸ C. Yuan

Laboratoire de l'Accélérateur Linéaire, Université de Paris-Sud, IN²P³-CNRS, F-91898 Orsay Cedex, France

G. Bagliesi, T. Boccali, L. Foà, A. Giammanco, A. Giassi, F. Ligabue, A. Messineo, F. Palla, G. Sanguinetti, A. Sciabà, R. Tenchini,¹ A. Venturi,¹ P.G. Verdini

Dipartimento di Fisica dell'Università, INFN Sezione di Pisa, e Scuola Normale Superiore, I-56010 Pisa, Italy

O. Awunor, G.A. Blair, G. Cowan, A. Garcia-Bellido, M.G. Green, L.T. Jones, T. Medcalf, A. Misiejuk, J.A. Strong, P. Teixeira-Dias

Department of Physics, Royal Holloway & Bedford New College, University of London, Egham, Surrey TW20 OEX, United Kingdom¹⁰

R.W. Clift, T.R. Edgecock, P.R. Norton, I.R. Tomalin

Particle Physics Dept., Rutherford Appleton Laboratory, Chilton, Didcot, Oxon OX11 0QX, United Kingdom¹⁰

B. Bloch-Devaux, D. Boumediene, P. Colas, B. Fabbro, E. Lançon, M.-C. Lemaire, E. Locci, P. Perez, J. Rander, B. Tuchming, B. Vallage

CEA, DAPNIA/Service de Physique des Particules, CE-Saclay, F-91191 Gif-sur-Yvette Cedex, France¹⁷

N. Konstantinidis, A.M. Litke, G. Taylor

Institute for Particle Physics, University of California at Santa Cruz, Santa Cruz, CA 95064, USA²²

C.N. Booth, S. Cartwright, F. Combley,³¹ P.N. Hodgson, M. Lehto, L.F. Thompson

Department of Physics, University of Sheffield, Sheffield S3 7RH, United Kingdom¹⁰

K. Affholderbach,²³ A. Böhler, S. Brandt, C. Grupen, J. Hess, A. Ngac, G. Prange, U. Sieler

Fachbereich Physik, Universität Siegen, D-57068 Siegen, Germany¹⁶

C. Borean, G. Giannini

Dipartimento di Fisica, Università di Trieste e INFN Sezione di Trieste, I-34127 Trieste, Italy

H. He, J. Putz, J. Rothberg

Experimental Elementary Particle Physics, University of Washington, Seattle, WA 98195 U.S.A.

S.R. Armstrong, K. Berkelman, K. Cranmer, D.P.S. Ferguson, Y. Gao,²⁹ S. González, O.J. Hayes, H. Hu, S. Jin, J. Kile, P.A. McNamara III, J. Nielsen, Y.B. Pan, J.H. von Wimmersperg-Toeller, W. Wiedenmann, J. Wu, Sau Lan Wu, X. Wu, G. Zobernig

Department of Physics, University of Wisconsin, Madison, WI 53706, USA¹¹

G. Dissertori

Institute for Particle Physics, ETH Hönggerberg, 8093 Zürich, Switzerland.

¹Also at CERN, 1211 Geneva 23, Switzerland.

²Now at Fermilab, PO Box 500, MS 352, Batavia, IL 60510, USA

³Also at Dipartimento di Fisica di Catania and INFN Sezione di Catania, 95129 Catania, Italy.

⁴Now at LBNL, Berkeley, CA 94720, U.S.A.

⁵Also Istituto di Cosmo-Geofisica del C.N.R., Torino, Italy.

⁶Now at Institut für Experimentelle Kernphysik, Universität Karlsruhe, 76128 Karlsruhe, Germany.

⁷Supported by CICYT, Spain.

⁸Supported by the National Science Foundation of China.

⁹Supported by the Danish Natural Science Research Council.

¹⁰Supported by the UK Particle Physics and Astronomy Research Council.

¹¹Supported by the US Department of Energy, grant DE-FG0295-ER40896.

¹²Now at Département de Physique Corpusculaire, Université de Genève, 1211 Genève 4, Switzerland.

¹³Supported by the Commission of the European Communities, contract ERBFMBICT982874.

¹⁴Supported by the Leverhulme Trust.

¹⁵Permanent address: Universitat de Barcelona, 08208 Barcelona, Spain.

¹⁶Supported by Bundesministerium für Bildung und Forschung, Germany.

¹⁷Supported by the Direction des Sciences de la Matière, C.E.A.

¹⁸Supported by the Austrian Ministry for Science and Transport.

¹⁹Now at SAP AG, 69185 Walldorf, Germany

²⁰Now at Groupe d' Astroparticules de Montpellier, Université de Montpellier II, 34095 Montpellier, France.

²¹Now at BNP Paribas, 60325 Frankfurt am Mainz, Germany

²²Supported by the US Department of Energy, grant DE-FG03-92ER40689.

²³Now at Skyguide, Swissair Navigation Services, Geneva, Switzerland.

²⁴Also at Dipartimento di Fisica e Tecnologia Relative, Università di Palermo, Palermo, Italy.

²⁵Now at McKinsey and Compagny, Avenue Louis Casal 18, 1203 Geneva, Switzerland.

²⁶Now at Honeywell, Phoenix AZ, U.S.A.

²⁷Now at INFN Sezione di Roma II, Dipartimento di Fisica, Università di Roma Tor Vergata, 00133 Roma, Italy.

²⁸Now at Centre de Physique des Particules de Marseille, Univ Méditerranée, F-13288 Marseille, France.

²⁹Also at Department of Physics, Tsinghua University, Beijing, The People's Republic of China.

³⁰Now at SLAC, Stanford, CA 94309, U.S.A.

³¹Deceased.

³²Also at Groupe d' Astroparticules de Montpellier, Université de Montpellier II, 34095 Montpellier, France.

³³Now at University of Florida, Department of Physics, Gainesville, Florida 32611-8440, USA

1 Introduction

Unlike at LEP 1 energies [1], ALEPH searches for the Standard Model Higgs boson at LEP 2 [2] were performed under the assumption that the Higgs boson decays predominantly into $b\bar{b}$. Invisible final states, which would arise for instance from a decay into a neutralino pair, were also investigated [2]. It is also possible, in the MSSM [3] as well as in more general two-Higgs-doublet models, to find parameter sets for which the decay into $b\bar{b}$ is strongly suppressed, to the benefit of other decay modes such as $c\bar{c}$, gg or $\tau^+\tau^-$. It is shown in this letter that either existing or slightly modified ALEPH searches for the Higgsstrahlung process $e^+e^- \rightarrow HZ$ are sensitive to these decays. These analyses are based on the 630 pb^{-1} of data collected by ALEPH between 1998 and 2000 at centre-of-mass energies ranging from 189 to 209 GeV (Table 1).

Table 1: Integrated luminosities, centre-of-mass energy ranges and mean centre-of-mass energy values for data collected by the ALEPH detector from 1998 to 2000.

Year	Luminosity (pb^{-1})	Energy range (GeV)	$\langle\sqrt{s}\rangle$ (GeV)
2000	11.2	207 – 209	208.0
	122.6	206 – 207	206.6
	80.0	204 – 206	205.2
1999	45.2	–	201.6
	86.3	–	199.5
	79.9	–	195.5
	28.9	–	191.6
1998	176.2	–	188.6

This letter is organized as follows. A brief description of the ALEPH detector is given in Section 2. The event selections pertaining to a flavour-independent search for the Higgs boson produced via the Higgsstrahlung process are examined in turn in Section 3, and the results are summarized in Section 4.

2 ALEPH Detector

A detailed description of the ALEPH detector and its performance can be found in Refs. [4] and [5]. The tracking system consists of a silicon vertex detector, a cylindrical drift chamber and a large time projection chamber (TPC), immersed in a 1.5 T axial magnetic field provided by a superconducting solenoidal coil. With these detectors, a transverse momentum resolution of $\delta p_t/p_t = 6 \times 10^{-4} p_t \oplus 5 \times 10^{-3}$ (p_t in GeV/c) is achieved.

An electromagnetic calorimeter placed between the TPC and the superconducting coil identifies electrons and photons, and measures their energies with a resolution of $\delta E/E = 0.18/\sqrt{E} + 0.009$ (E in GeV). The iron return yoke is instrumented with 23 layers

of streamer tubes and serves as a hadron calorimeter and muon filter. Two additional double layers of streamer tubes outside the return yoke aid the identification of muons.

An energy flow algorithm [5] combines the information from the tracking detectors and the calorimeters and provides a list of reconstructed charged and neutral particles. The achieved energy resolution is $\sigma(E) = 0.6\sqrt{E} + 0.6$ (E in GeV).

3 Event selections

In this analysis, decays of the Higgs boson to hadrons or to tau pairs are considered. Hadronic Higgs boson decays are searched for in four-jet, missing-energy and leptonic (electron or muon pair) final states as for the Standard Model search for the $e^+e^- \rightarrow HZ$ process. The event selections used here for the missing energy and leptonic final states are based on those used in the previous searches [6, 7], however without b-tagging information. A specially designed flavour-independent selection is used for the four-jet channel. Higgs boson decays to a tau pair are searched for in the final state $\tau^+\tau^-q\bar{q}$, using the same selection described in Ref. [7].

Signal efficiencies and background contributions from Standard Model processes are estimated with simulated event samples which include a full simulation of the ALEPH detector. To study the signal efficiency for $H \rightarrow$ hadrons, events from the HZ process are generated in which the H decays to $b\bar{b}$, $c\bar{c}$ or gg and the Z into a pair of quarks, neutrinos, electrons or muons. Events in which H decays to a pair of taus and the Z to a pair of quarks are used to determine the tau channel efficiency. Signal events are simulated with the Monte Carlo generator HZHA [8], for m_H from 40 to 115 GeV/ c^2 in steps of 5 GeV/ c^2 . The simulated background event samples are identical to those used in Ref. [6].

3.1 Leptonic and missing energy final states

The leptonic channel event selection, which does not include b-tagging information, is unchanged with respect to Ref. [6]. The reconstructed Higgs boson mass, computed as the mass recoiling against the lepton system, is used as a discriminant variable in the confidence level calculation. When this analysis is applied to the data [2, 7, 10], 70 events are observed, in agreement with the 73.4 events expected from the Standard Model backgrounds. The signal efficiencies for $H \rightarrow b\bar{b}$, $c\bar{c}$ or gg are found to be quite similar, at about 80% over the entire mass range, except when approaching the kinematic limit for HZ production where it falls to 40%.

As for the leptonic analysis, the Standard Model missing energy event selection applied to data collected in 2000 does not include b-tagging information, and is therefore used in this search. In this analysis, the reconstructed Higgs boson mass is used as a discriminant variable in the confidence level calculation. Prior to 2000, the Standard Model missing energy event selections relied explicitly on b tagging, and are therefore inappropriate for this analysis. A modified version of the three-neural-network analysis described in Ref. [7] is applied to this data sample. This analysis uses the seven-variable anti- $q\bar{q}$ and three-variable anti- WW neural networks used in the standard analysis. When these analyses are applied to the data, 177 events

are selected in the sample with 181 expected from Standard Model background processes. Cuts on the two neural network outputs are chosen to optimize the search sensitivity as a function of the Higgs boson mass. The signal efficiencies for $H \rightarrow b\bar{b}$, $c\bar{c}$ or gg are found to be quite similar, and are about 40% over the entire mass range, falling to 20% near the kinematic limit.

3.2 Final state with taus

The search for the $\tau^+\tau^-\text{q}\bar{\text{q}}$ final state of Ref. [6] is used here for Higgs bosons decaying into tau pairs. The selection efficiency is around 40%. The reconstructed Higgs boson mass is used as a discriminant variable in the confidence level calculation. A total of 27 candidate events is selected in the data, in agreement with 27.2 expected from background processes.

3.3 Four-jet final state

The preselection of the flavour-independent four-jet selection is similar to that of the standard four-jet analysis [10]. Events are required to have at least eight charged particle tracks, and the total energy of the charged particles must be larger than 10% of the centre-of-mass energy. Events from radiative returns to the Z resonance, in which a photon escapes undetected down the beam pipe, are rejected by requiring the momentum p_z of the event along the beam axis to satisfy $p_z < 1.5(m_{\text{vis}} - 90)$, where m_{vis} is the total visible mass in the event, expressed in GeV/c^2 . Events are then clustered into four jets using the Durham jet-clustering algorithm [9]. The transition from four to three jets is required to occur for $y_{34} > 0.008$. Events from radiative returns to the Z with a photon in the detector are rejected if more than 80% of the energy of any jet is in the form of electrons and photons. Events from semileptonic decays of W^+W^- are rejected by requiring that the energy of the most energetic identified electron or muon is less than 20 GeV. To avoid overlap with the leptonic selection, events containing a pair of identified electrons or muons with an invariant mass greater than $40 \text{ GeV}/c^2$ are rejected. After this preselection, signal efficiencies for $H \rightarrow b\bar{b}$, $c\bar{c}$ and gg are of the order of 70%. The numbers of events expected from background processes and the numbers of candidate events observed in the data are reported in Table 2. The comparison indicates a reasonable agreement between data and the expectation from Standard Model processes at the preselection level.

This analysis uses several of the kinematic variables used in the standard analysis and in addition, three variables based on di-jet mass information:

- the significance of the distance to the W^+W^- hypothesis, defined as

$$\mathcal{E}_{\text{WW}} = \min_{i,j,k,l=1,4} \{ (m_{ij} + m_{kl} - 2m_W)^2 / \sigma_s^2 + (m_{ij} - m_{kl})^2 / \sigma_d^2 \},$$

where $\sigma_s = 4 \text{ GeV}/c^2$ and $\sigma_d = 10 \text{ GeV}/c^2$ are the resolutions on the sum and the difference of the di-jet masses for W^+W^- production, and i, j, k, l denote the four jets reconstructed in the event;

Table 2: Numbers of expected events from background processes and numbers of candidate events collected at centre-of-mass energies from 189 to 209 GeV, at the preselection level for the four-jet final state selection.

\sqrt{s} (GeV)	Background process contributions				Data
	WW	q \bar{q}	ZZ	Total	
188.6	1002.1	261.5	63.8	1327.5	1242
191.6	165.2	41.9	11.8	218.9	221
195.5	459.8	108.1	35.7	603.4	614
199.5	492.3	108.0	40.0	640.1	624
201.6	238.9	51.2	19.7	309.7	261
204–209	1251.0	247.9	102.8	1601.6	1601
All \sqrt{s}	3609.3	818.6	273.8	4701.7	4563

- the probability density functions $\mathcal{S}_{m_H}(\mathcal{E}_{\text{HZ}})$ and $\mathcal{B}_{m_H}(\mathcal{E}_{\text{HZ}})$ for signal and background. Here, \mathcal{E}_{HZ} is the significance of the distance to the HZ hypothesis. It depends on m_H and is defined as

$$\mathcal{E}_{\text{HZ}} = \min_{i,j,k,l=1,4} \left\{ \frac{[(m_{ij} + m_{kl}) - (m_Z + m_H)]^2}{\sigma_\Sigma^2} + \frac{[(m_{ij} - m_{kl}) - (m_H - m_Z)]^2}{\sigma_\Delta^2} \right\},$$

where σ_Σ and σ_Δ are the resolutions on the sum and the difference of di-jet masses for HZ production. Simulated event samples are used to parametrize \mathcal{S}_{m_H} and \mathcal{B}_{m_H} .

These three variables are combined with the smallest jet energy E_{jet}^{\min} , the largest jet energy E_{jet}^{\max} , and the product $E_{\text{jet}}^{\min}\theta_{ij}$ of the smallest jet energy and the minimum angle between any two jets, in a six-variable neural network. In order to optimize the performance over a wide range of masses, separate neural networks are trained for several Higgs boson mass hypotheses, ranging from 40 to 115 GeV/ c^2 , in steps of 5 GeV/ c^2 , at three different centre-of-mass energies : 189, 199.5 and 206.7 GeV. For each of these networks, an optimization using the \bar{N}_{95} [11] prescription is performed to determine the appropriate cut for the neural network output. As the di-jet mass information is included in the neural network, it is not included again as a discriminant variable when computing the confidence level.

As neural networks are trained every 5 GeV/ c^2 , a sliding method is used to determine the selection at intermediate Higgs boson masses. For a mass m_H intermediate between two training masses m_1 and m_2 , \mathcal{S}_{m_H} (\mathcal{B}_{m_H}) is interpolated from \mathcal{S}_{m_1} (\mathcal{B}_{m_1}) and \mathcal{S}_{m_2} (\mathcal{B}_{m_2}). These quantities are input to the network trained at m_1 and to the network trained at m_2 . The two neural networks outputs are then interpolated to calculate NN_{m_H} . The cut value on NN_{m_H} , the signal efficiency and background expectation at the intermediate mass are similarly obtained by interpolations. The validity of this procedure has been established with test samples of signal events simulated at $\sqrt{s} = 199.5$ GeV for masses between 60 and 100 GeV/ c^2 in steps of 1 GeV/ c^2 .

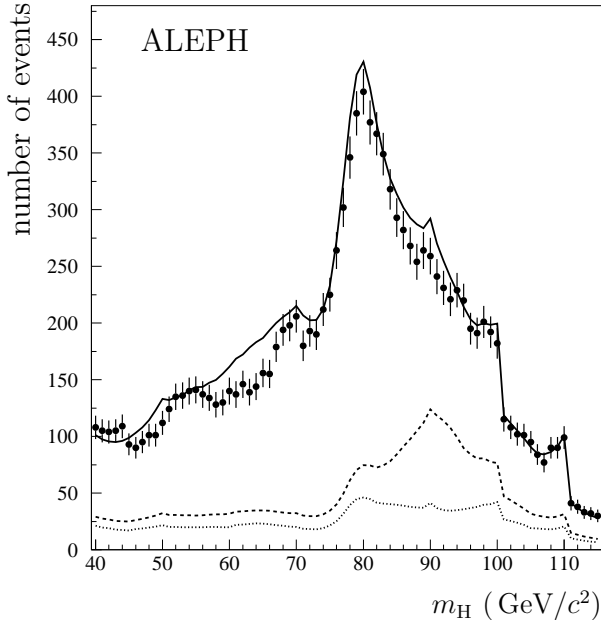


Figure 1: Expected background (solid curve) compared to collected data (dots) by the four-jet selection as a function of the Higgs boson mass hypothesis at centre-of-mass energies from 189 to 209 GeV. The dotted curve represents the contribution from the $q\bar{q}$ background and the dashed curve represents the additional contribution from the ZZ background.

The number of events selected by this analysis in data is compared to the background expectation in Fig. 1 as a function of the Higgs boson mass hypothesis. The points are statistically correlated, as mass resolution effects usually allow the events to contribute to several adjacent mass bins. As a result, a deficit in one mass region can be propagated to a large range of mass hypotheses, as observed in the 60 and 90 GeV/c^2 regions, correlated to the W^+W^- and ZZ deficits already described in Ref. [10] and Ref. [12].

4 Results

In every channel under investigation, no departure from Standard Model expectations consistent with the presence of a Higgs signal is observed in the data. Lower limits on the lightest scalar Higgs boson mass are derived as a function of ξ_{had}^2 or ξ_τ^2 , the product of the branching fraction to either hadronic jets or tau pairs and of the ratio of the production cross section to the Standard Model production cross section. In order to obtain a flavour-independent limit for the decay $H \rightarrow \text{hadrons}$, the smallest of the signal efficiencies for $H \rightarrow b\bar{b}$, $c\bar{c}$ and gg is used at each Higgs boson mass hypothesis. For a Higgsstrahlung cross section equal to that of the Standard Model and for 100% branching fraction to hadrons, Higgs boson masses below 110.6 GeV/c^2 are excluded at 95% C.L., where a limit of 110.5 GeV/c^2 is expected in the absence of signal.

When the parameter ξ_{had}^2 is allowed to vary, the result of the flavour-independent search is

expressed as an excluded domain in the $(m_H, \xi_{\text{had}}^2)$ plane, as shown in Fig. 2a. Results from Ref. [13] are used to exclude Higgs boson mass hypotheses below $40 \text{ GeV}/c^2$.

A similar procedure is followed to obtain a limit on the decay $H \rightarrow \tau^+\tau^-$, and the exclusion in the (m_H, ξ_τ^2) plane is shown in Fig. 2b. For $\xi_\tau^2 = 1$, a lower limit on the Higgs boson mass of $112.4 \text{ GeV}/c^2$ at 95% C.L. is obtained, where a limit of $113.9 \text{ GeV}/c^2$ is expected in the absence of signal. Under the assumption that $\xi_{\text{had}}^2 + \xi_\tau^2 = 1$, a $109.1 \text{ GeV}/c^2$ lower limit on m_H is obtained irrespective of ξ_τ^2 .

The dominant systematic error sources, evaluated as described in Ref. [7], are included in the obtained limits. The finite size of the simulated event samples, the jet energy and angular resolutions and the uncertainties in the signal and background cross section estimations affect all the topologies under investigation. In the leptonic channel, lepton identification and isolation are additional sources of uncertainty. For the four-jet channel, systematic uncertainties due to differences between data and simulation in the event selection variables are taken into account with an event reweighting method [14]. The global effect of these uncertainties is to decrease the hadronic limit by $190 \text{ MeV}/c^2$, and the tau limit by $10 \text{ MeV}/c^2$.

5 Conclusions

In order to explore nonstandard Higgs scenarios, searches for Higgs bosons produced via Higgsstrahlung decaying to hadrons and to tau leptons were performed. The selections are similar to those used in previous searches, except for the search in the four-jet final state, where a new analysis was designed in order to cope with hadronic Higgs boson decays without a flavour tag. No evidence of Higgs boson production is observed in the search for either hadronic or tau decays in the data collected at energies between 189 and 209 GeV. For a Standard Model Higgsstrahlung cross section and a 100% branching fraction to hadrons, masses below $110.6 \text{ GeV}/c^2$ are excluded at 95% C.L. independent of the flavour of the Higgs boson decay. Results on flavour-independent Higgs boson production have also been reported by the OPAL collaboration [15] with lower energy data. For a Standard Model Higgsstrahlung cross section and a 100% branching fraction to $\tau^+\tau^-$, masses below $112.4 \text{ GeV}/c^2$ are excluded at 95% C.L..

Acknowledgements

We congratulate our colleagues from the accelerator divisions for the very successful running of LEP at high energies. We are indebted to the engineers and technicians in all our institutions for the excellent performance of ALEPH. Those of us from non-member countries thank CERN for its hospitality.

References

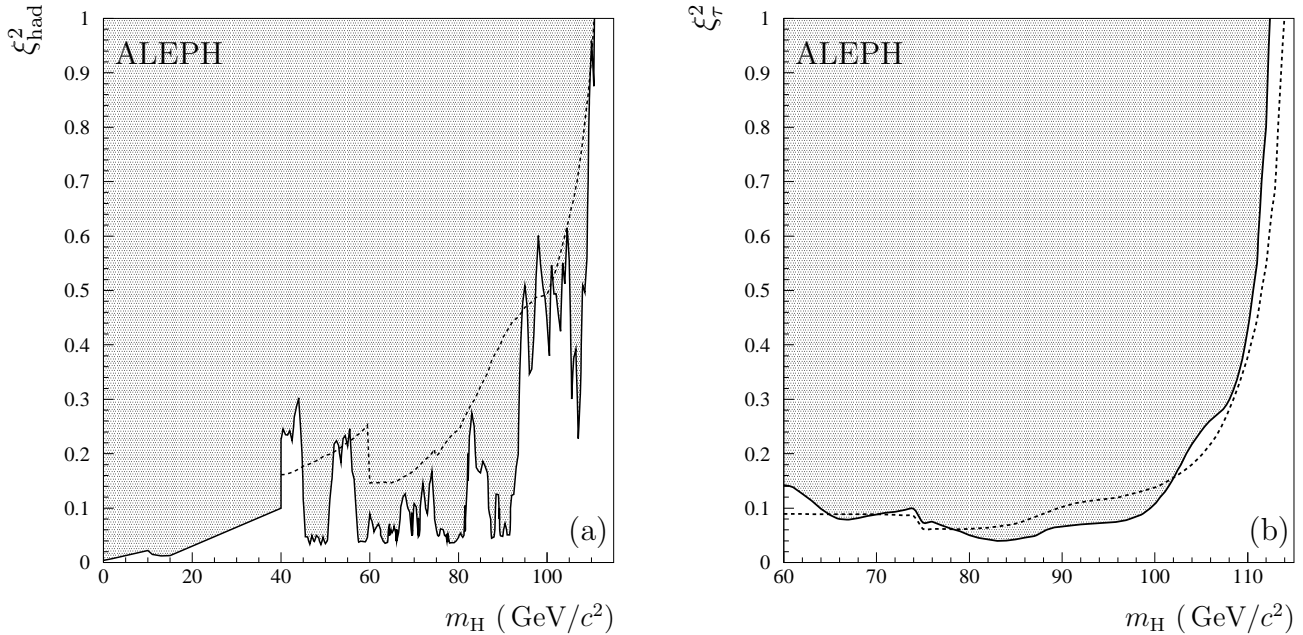


Figure 2: Expected (dashed line) and observed (shaded area) 95% C.L. limits on a) ξ_{had}^2 and b) ξ_τ^2 , as a function of the Higgs boson mass hypothesis and for centre-of-mass energies up to 209 GeV.

- [1] ALEPH Collaboration, *Mass limit for the Standard Model Higgs Boson with the full LEP 1 ALEPH Data Sample*, Phys. Lett. **B384** (1996) 427.
- [2] ALEPH Collaboration, *Final results of the ALEPH Searches for neutral Higgs Bosons*, Phys. Lett. **B526** (2002) 191.
- [3] M. Carena, S. Heinemeyer, C.E.M. Wagner and G. Weiglein, *Suggestions for improved benchmark scenarios for Higgs bosons searches at LEP 2*, CERN-TH/99-374 (1999).
- [4] ALEPH Collaboration, *ALEPH: a detector for electron-positron annihilation at LEP*, Nucl. Instrum. and Methods **294** (1990) 121.
- [5] ALEPH Collaboration, *Performance of the ALEPH detector at LEP*, Nucl. Instrum. and Methods **A360** (1995) 481.
- [6] ALEPH Collaboration, *Observation of an excess in the search for the Standard Model Higgs boson at ALEPH*, Phys. Lett. **B495** (2000) 1.
- [7] ALEPH Collaboration, *Search for the neutral Higgs bosons of the Standard Model and the MSSM in e^+e^- collisions at $\sqrt{s} = 189$ GeV*, Eur. Phys. J. **C17** (2000) 223.
- [8] P. Janot, *The HZHA generator*, in “Physics at LEP”, Eds. G. Altarelli, T. Sjöstrand and F. Zwirner, CERN 96-01 (1996), Vol. 2, p. 309.
- [9] S. Catani *et al.*, *New clustering algorithm for multi-jet cross sections in e^+e^- annihilation*, Phys. Lett. **B269** (1991) 179;

- N. Brown, W.J. Stirling, *Finding jets and summing soft gluons : A new algorithm*, Z. Phys.C 53 (1992) 629.
- [10] ALEPH Collaboration, *Searches for neutral Higgs bosons in e^+e^- collisions at centre-of-mass energies from 192 to 202 GeV*, Phys. Lett. **B499** (2001) 53.
- [11] J.-F. Grivaz, F. Le Diberder, *Complementary analyses and acceptance optimisation in new particle searches*, LAL 92-37;
ALEPH Collaboration, *Search for the Standard Model Higgs boson*, Phys. Lett. **B313** (1993) 299.
- [12] ALEPH Collaboration, *Measurement of W -pair production in e^+e^- collisions at 189 GeV*, Phys. Lett. **B484** (2000) 205.
- [13] ALEPH Collaboration, *Search for non-minimal Higgs boson produced in the reaction $e^+e^- \rightarrow hZ^*$* , Phys. Lett. **B313** (1993) 312.
- [14] ALEPH Collaboration, *Searches for the Standard Model Higgs boson at the LEP2 collider near $\sqrt{s} = 183$ GeV*, Phys. Lett. **B447** (1999) 336.
- [15] OPAL Collaboration, *Two Higgs doublet model and model independent interpretation of neutral Higgs boson searches*, Eur. Phys. J. **C18** (2001).